JOURNAL OF CATALYSIS 76, 208–224 (1982)

The Characterization of Carbon-Supported Iron Catalysts: Chemisorption, Magnetization, and Mössbauer Spectroscopy

H-J. JUNG,* M. A. VANNICE,* L. N. MULAY,† R. M. STANFIELD,‡ AND W. N. DELGASS‡

*Department of Chemical Engineering and †Department of Material Sciences and Engineering, The Pennsylvania State University, University Park, Pennsylvania 16802, and ‡School of Chemical Engineering, Purdue University, West Lafayette, Indiana 47907

Received November 2, 1981; revised February 24, 1982

Chemisorption, Mössbauer effect, kinetics, and magnetic studies have been combined to characterize iron on V3G, a low surface area graphitic carbon, and on Carbolac-1, a porous, high surface area carbon black. Magnetic studies confirm the conducting, graphitic properties of V3G and the insulating, amorphous properties of Carbolac-1. All techniques show the iron on V3G to be in large particles which show ferromagnetic behavior. The iron on Carbolac-1 is highly dispersed, shows superparamagnetism and oxidation sensitivity characteristic of very small particles, and exhibits a decreased reducibility suggestive of a support interaction. These small iron particles show greatly decreased H_2/CO chemisorption ratios at temperatures up to 473 K, a high olefin to paraffin ratio, and excellent activity maintenance during Fischer–Tropsch synthesis.

INTRODUCTION

Although iron is the catalyst presently used in commercial Fischer–Tropsch processes, significant improvements in selectivity and activity maintenance would be highly desirable. Unsupported, doubly promoted iron is currently in use, and few studies on supported iron as Fischer–Tropsch catalysts have been reported even though such systems could offer better activity maintenance, different selectivities, and higher throughput per unit volume as a consequence of higher dispersions and/or metal–support interactions. Recent studies on carbon-supported iron have shown that such systems are very active and possess noticeably different selectivities compared to alumina-supported iron (*1*, *2*). Highly dispersed (HD) Fe/C catalysts were prepared as well as catalysts with low dispersion. The former group was found to exhibit a much higher olefin/paraffin ratio, improved activity maintenance, and turnover frequencies over an order of magnitude lower than those on large iron particles (*1*, *2*).

In addition, these reduced Fe/C catalysts exhibited complex chemisorption behavior at 300 K—hydrogen chemisorption either did not occur or was very low while CO chemisorption always occurred. In some cases very large CO uptakes indicated the presence of very small iron particles (i.e., high dispersions). The chemisorption studies divided the iron/carbon catalysts into two general groups: Those with high dispersion (HD) and those with low dispersion (LD) (*2*). To verify preparation of well-dispersed iron, and to help determine if the changes in catalytic properties were due primarily to a crystallite size effect or to an interaction between the iron and the carbon, a representative catalyst from each group was chosen for more thorough characterization. Five percent Fe/C-1 (Carbolac-1) from the HD group and 4.5% Fe/V3G (Vulcan 3 graphite) from the LD group were studied by magnetization techniques, Mössbauer spectroscopy, and additional chemisorption studies from 195 to 373 K. These results are reported here. To the best of our knowledge, the only other study to characterize a supported iron catalyst so

0021-9517/82/070208-17$02.00/0
Copyright © 1982 by Academic Press, Inc.
All rights of reproduction in any form reserved.

thoroughly is that of Boudart *et al.*, who found good agreement among all three techniques for MgO-supported iron (*3*).

EXPERIMENTAL

A. Catalyst preparation and materials. The preparation of catalysts used in this work has been described previously (*1, 2*). Briefly, the two catalysts of primary interest, 5% Fe/C-1 and 4.5% Fe/V3G, were prepared by wetting Carbolac-1 (C-1) and Vulcan 3 Graphite (V3G), respectively, with an aqueous solution of iron nitrate [$Fe(NO_3)_3 \cdot 9H_2O$ from Baker Chemical Co.]. The Carbolac-1 is a relatively porous carbon black from Cabot Corporation and has a total specific surface area of 950 $m^2\ g^{-1}$. The Vulcan 3 Graphite, obtained after graphitizing the nonporous Vulcan 3 carbon black (from Cabot) at 3073 K, has a surface area of 56 $m^2\ g^{-1}$.

Two different samples of 5% Fe/C-1 were prepared. Sample 1 was used in preceding studies (*1, 2*) and Sample 2 was prepared during this investigation. All studies in this paper were conducted only on Sample 1 with the exception of the chemisorption results, which were conducted on both samples.

The gases used, He (Matheson—99.9999% purity), H_2 (Matheson—99.999% purity), and CO (Matheson—99.99% purity), were further purified. The He was passed through a Dryrite-molecular-sieve trap (Alltech Assoc., Inc.) and then through an Oxy-trap (Alltech Assoc., Inc.). The H_2 was passed through a Deoxo unit (Engelhard Ind.), a 5 A molecular sieve trap, and finally through an Oxy-trap. The CO was passed through a 5 A molecular sieve trap at 195 K.

B. Chemisorption measurements. CO and hydrogen uptakes were measured in a mercury-free, glass volumetric adsorption system which has been described previously (*2*). An ultimate vacuum of 7×10^{-5} Pa (5×10^{-7} Torr) could be achieved. Pressures in the adsorption cell were measured with a Texas Instruments Precision Pressure Gage. Unless otherwise noted, all samples were reduced for 16 hr in flowing H_2 at 673 K followed by a 1 hr evacuation at 648 K before cooling under dynamic vacuum to the desired temperature.

C. Kinetic measurements. Kinetic studies were conducted in a small, glass, plug-flow reactor which has been described in detail previously (*1, 2*). Product analyses were performed using a Perkin-Elmer Data Analyzer and a P-E Sigma 3 gas chromatograph with subambient temperature programming and Chromosorb 102 columns. Catalyst charges to the reactor were 1 g or less and conversions near 5% or lower were maintained so that the reactor operated in a differential mode. Kinetic data were obtained after a 20-min period onstream following a 20-min exposure to pure H_2 (*4*). All samples, unless otherwise noted, were reduced for 16 hr at 673 K in 50 $cm^3\ min^{-1}$ H_2 before cooling in H_2 to the desired temperature.

D. Magnetic measurements. The magnetization per gram (σ in emu g^{-1}) of the samples was measured using a modified Faraday method (*5, 6*) with the aid of a vacuum/gas-handling system. The static field H was calibrated with a Hall-probe gauss-meter (Bell, Inc.). A few milligrams of the sample was placed in a small quartz bucket (~5 mm o.d., ~5 mm tall) which was suspended from the central position of the Cahn R. G. electrobalance beam into the flow-through hangdown chamber. Details of the design of the hangdown tube, the electromagnet, and the pole-pieces are described in the literature (*6*). The water-cooled electromagnet provided variable fields up to 8 kOe with a field gradient, $H \cdot dH/dx$, which was constant over a 4-cm region. The vacuum/gas-handling system was arranged so that the sample could be reduced *in situ* in flowing H_2 and readily outgassed to 7×10^{-4} Pa.

The Faraday balance was calibrated using for reference MTC (Mercury tetrathiocyanatocobaltate II), $Hg[Co(CNS)_4]$ which has a mass susceptibility, χ_g, of 16.44 $\times$

10^{-6} cm^3 g^{-1} (or "emu" g^{-1}) at 293 K. This corresponds to a susceptibility of 2.07×10^{-7} m^3 kg^{-1} in SI units. The performance of the balance was checked by measuring the susceptibility (in emu g^{-1}) of a standard diamagnetic solid such as $CuSO_4$ ($\chi_{meas} = 7.9 \times 10^{-6}$, $\chi_{literature} = 8.3 \times 10^{-6}$). A compilation of standard values for the susceptibility of several diamagnetic and paramagnetic compounds and conversion factors from emu/g to SI units is given elsewhere (*7*).

The standard pretreatment procedure included a stepwise reduction of the catalyst for a desired period of time at 673 K in an H_2 flow of 100 cm_{stp}^3 min^{-1} (*2*). The sample was then outgassed for 1 hr at 650 K, and cooled to 80, 195, or 295 K, the measurement temperature. A small amount of He was added to facilitate the cooling.

E. Mössbauer spectroscopy. The Austin Science Associates constant acceleration Mössbauer spectrometer and high temperature absorber cell used in this work have been described elsewhere (*8, 9*). The source was 50 mCi of ^{57}Co diffused into a Rh matrix (Amersham Corp.), but all Mössbauer spectra presented here have zero isomer shift referenced to a 25 μm NBS Fe foil. A multipurpose gas handling system described in Ref. (*8*) allowed evacuation of the absorber cell to 1.3×10^{-3} Pa and flow at one atmosphere of H_2, O_2, He, or synthesis gas ($H_2/CO = 3.3$). All gases were UHP grade from Matheson with the H_2 and synthesis gas being further purified by passage through an Engelhard Deoxo 10 ft^3/hr capacity oxygen–hydrogen catalytic purifier and a subsequent bed of 5A and 13X molecular sieves to remove water.

The Mössbauer spectra were computer fitted to Lorentzian lineshapes by a variable metric minimization program. Linear constraints were applied when close overlaps of lines led to nonphysical fitted parameters from unconstrained fits. In general, when magnetically split components accounted for less than 15% of the total spectral area, the widths of the six lines were set equal, intensities constrained to the expected 3 : 2 : 1 : 1 : 2 : 3 ratios, and in some cases, the relative positions fixed at expected values. Iron oxide doublets with low intensities were given equal widths and, if necessary, equal dips. Overlap problems such as that in spectrum 3b, were solved by constraining the fourth Fe° peak to have a width equal to that of the third and intensity $\frac{1}{3}$ that of the sixth peak. The solid lines drawn through the Mössbauer data correspond to the fitted parameters in Tables 3 and 4.

RESULTS AND DISCUSSION

A. Chemisorption Behavior

The pioneering work of Emmett and coworkers was directed predominantly toward unsupported, singly and doubly promoted iron catalysts (*10*), and few studies since have examined CO and H_2 adsorption on pure iron. Recent UHV studies by Wedler *et al.* on iron films showed clearly that both H_2 and CO adsorb rapidly at 273 K, and coverages became essentially pressure-independent above 10^{-2} Pa (*11, 12*). Other UHV studies of CO adsorption on the close-packed (110) surface (*13*) and the (100) plane (*14*) show that slow dissociation can occur after molecular adsorption at temperatures near 300 K. Only dissociative adsorption was observed on the rough Fe(111) surface at 300 K (*15*). At higher temperatures, more rapid CO dissociation occurred. Thorough studies on MgO-supported iron have also shown that CO adsorbs readily on reduced iron surfaces (*3*), but activated H_2 adsorption requiring high temperatures for high coverage occurred on small iron crystallites (<10 nm) (*16*).

Although standard gas chemisorption techniques do not exist for iron (*17*) and the adsorption stoichiometry of CO might be expected to vary from 1 to 2 (*3*), good agreement among different techniques to measure particle size has been obtained assuming a ratio of 1 CO : 2 Fe_s (*3*), where Fe_s represents a surface Fe atom. The CO che-

TABLE 1

Chemisorption at Different Temperatures on Carbon-Supported Iron Catalysts

Catalyst	Temperature (°K)	Gas uptake (μmole g^{-1})		CO/Fe	H/Fe	d^a (nm)
		CO	H_2			
4.5% Fe/V3G[b]	195	10.0	3.6	0.012	0.0089	30
	300	5.4	2.5	0.0067	0.0062	56
	373	3.6	7.0	0.0045	0.017	84
5% Fe/C-1						
Sample 1[c]	195	127	4.6	0.14	0.010	2.7
	300	400	3.1	0.45	0.0069	1.0
	373	—	5.0	—	0.011	—
5.0% Fe C-1						
Sample 2[d]	195	145	4.6	0.16	0.010	2.3
	300	500	5.9	0.56	0.013	<1.0
	373	150	12.2	0.17	0.027	2.2
	473	168	—	0.19	—	2.0

[a] Assuming CO : Fe_S = 1 : 2.
[b] Reduced 13.5 hr at 673 K.
[c] Reduced 18 hr at 673 K.
[d] Reduced 16 hr at 673 K.

misorption results in Table 1 clearly show that the preparation of small iron particles on C-1 is reproducible, as Sample 2 had even higher uptakes than Sample 1, and that large iron particles exist in 4.5% Fe/V3G, regardless of choice of adsorption stoichiometry. Even if CO adsorption shifted from bridged to linear on small iron particles, crystallite sizes would be only double those calculated in Table 1. Adsorption blanks were run on the pure carbon supports and no irreversible adsorption occurred at any temperature (*18*). The average particle sizes, d, were calculated using the equation $d(\text{nm}) = C/D$ with $C = 0.75$ nm and $D = Fe_s/Fe_t$ where Fe_t is the total number of Fe atoms. The value of C is obtained using 0.094 nm^2 per Fe_s atom (*19*).

The reproducibility of high CO uptakes on 5% Fe/C-1, particularly at 300 K, is clearly shown by the agreement here and with previous results (*1, 2*). Table 1 shows that CO uptakes on both 5% Fe/C-1 and 4.5% Fe/V3G seem to be dependent on temperature but the trends are clearly different. The behavior on 4.5% Fe/V3G is that expected for an equilibrated, exothermic process, whereas uptakes triple on the 5% Fe/C-1 catalyst at 300 K compared to 195 K.

Although the behavior for the 5% Fe/C-1 is unusual, it is consistent with the presence of small Fe crystallites. The formation of subcarbonyl species apparently can occur on highly dispersed Ru, Rh, and Ni (*20*) and because iron can form various carbonyls, similar behavior is not unexpected for very small Fe particles. Subcarbonyl formation is not expected on large metal crystallites. Subcarbonyl formation is suggested here because the assumption of a CO/Fe_s ratio of 0.5 at 195 K gives a CO/Fe_s ratio of 1.7 at 300 K, and the presumption of linear adsorption at 195 K produces a ratio near 3.5 at 300 K. The rapid decrease in CO uptake as temperatures increase to 373 K and higher is almost certainly due to destruction of the subcarbonyl species followed by CO dissociation, the former of which should be very temperature sensitive. The excellent agreement in uptakes at 195 and 373 is consistent with our argument because bridged-bonded adsorption and dissociative adsorption would produce identical uptakes of

irreversibly adsorbed CO in the absence of any complications such as bulk oxidation.

Hydrogen adsorption on iron is a complicated process and adsorption is expected to be more meaningful at 373 K than the lower temperatures (*10, 16*). The study of Topsøe *et al.* (*16*), reported after the completion of this work, indicated that 473 K is preferred; however, there is reasonable agreement between CO adsorption at 195 K and H_2 adsorption at 373 K on the large Fe crystallites, and these results on 4.5% Fe/V3G are in agreement with studies on pure bulk iron (*18*). In contrast, hydrogen uptakes remain greatly suppressed up to 373 K on the 5.0% Fe/C-1, which is consistent with the recent study of Topsøe *et al.* which found hydrogen chemisorption to be activated up to 473 K on small Fe particles dispersed on MgO (*16*). This would account for the very low H_2/CO uptake ratios over the temperature range utilized in this study. Typical isotherms for H_2 and CO adsorption are shown elsewhere (*18*).

B. Diamagnetic Susceptibility of the Pure Carbon Supports and the Degree of Graphitization

The mass susceptibility (χ) per gram of the carbon supports was measured as a function of the field so that the Honda–Owen method (*21, 22*) could be used to obtain the true susceptibility (χ_t) value for the carbon support. The Honda–Owen relation is

$$\chi = \chi_t + \frac{\omega\sigma_S}{H} \qquad (1)$$

where ω refers to the amount of a ferromagnetic impurity per gram of carbon and σ_S is the saturation magnetization per gram of the ferromagnetic impurity. Equation (1) shows that the true susceptibility (χ_t) for the carbon support and the amount of the ferromagnetic impurity in the carbon support can be estimated from the intercept and slope of a plot of χ versus $1/H$. The susceptibility data for the carbon supports were needed not only to elucidate the electronic properties of the support itself, but also to obtain the magnetization per gram of the iron in the catalyst sample, σ_{Fe} ($= \chi_{Fe} \cdot H$), using Wiedemann's additivity law (*5*):

$$\chi_{catalyst} = W\chi_{Fe} + (1 - W)\chi_{support} \qquad (2)$$

where $\chi_{catalyst}$, χ_{Fe}, and $\chi_{support}$ are the mass susceptibilities of the catalyst, the metal (iron), and the support, respectively, and W refers to the weight fraction of iron in the catalyst.

The χ values for Carbolac-1 (C-1) and Graphitized Vulcan 3 (V3G) measured at room temperature as a function of field (H) are plotted versus $1/H$ in Fig. 1. For C-1, the χ values increased noticeably as reduction time in H_2 at 673 K increased, and at higher fields they were linearly dependent on the reciprocal of the field ($1/H$). This behavior clearly shows the presence of ferromagnetic impurities in the sample, and is in agreement with the spectroscopic analysis shown in Table 2. This analysis reveals that C-1 is a relatively pure carbon black containing about 180 ppm of iron as the only ferromagnetic impurity and about 270 ppm of various para- and diamagnetic impurities. No activity for CO hydrogenation was found over pure C-1, showing that the impurities did not contribute to the catalytic activity of 5.0% Fe/C-1. Using the method of Honda and Owen (*21, 22*), the amount of the ferromagnetic impurity in Carbolac-1 was estimated to be 108 ppm, which is low but in reasonable agreement with the spectroscopic analysis (183 ppm Fe). Taking the average of the measured χ_t values at reduction times from 0 to 11 hr, a value of -0.1 (± 0.03) $\times 10^{-6}$ emu g^{-1} is obtained for pure C-1.

The V3G sample, on the other hand, exhibited a field independence of susceptibility which is typical of a normal diamagnetic material and indicates that the sample did not contain any ferromagnetic impurities. The value of χ_t for V3G is about -6.3×10^{-6} emu g^{-1}, independent of reduction treatment. It is known that graphitization of a carbon black to give a mean diameter, L_a,

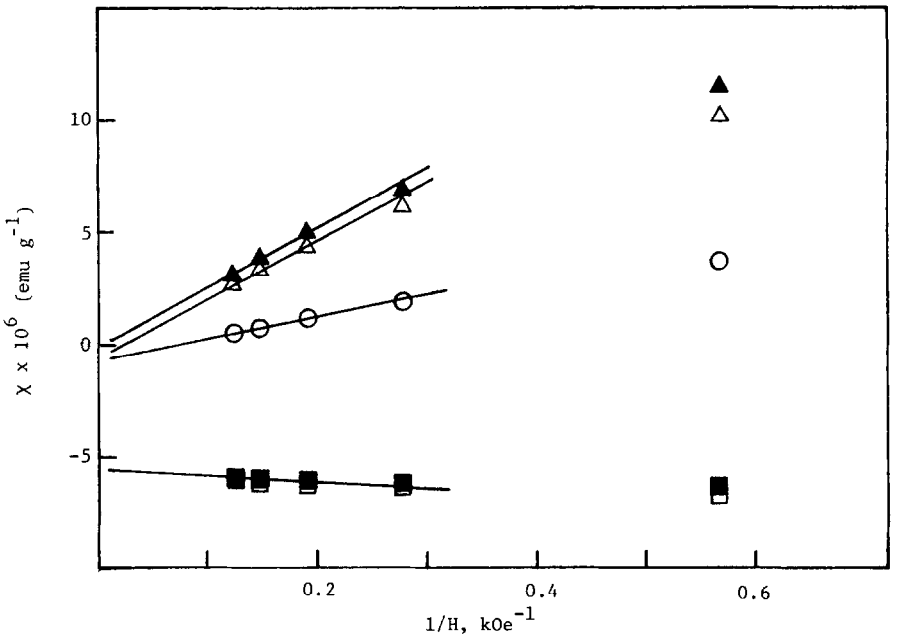

FIG. 1. Diamagnetic susceptibility of carbons as a function of reciprocal magnetic field at 295 K. □, V3G-unreduced; ■, V3G reduced 1 hr; ○, C-1 unreduced; △, C-1 reduced 1 hr; ▲, C-1 reduced 11 hr.

of the basal planes of approximately 6 nm, produces a change in the mean diamagnetic susceptibility from about -0.85×10^{-6} to -6.5×10^{-6} emu g^{-1} (*23*). The measured true susceptibility values for the amorphous C-1 carbon black and the graphitized V3G carbon black agree well with these values. The susceptibility value of C-1, which seems less diamagnetic, or even slightly paramagnetic, compared to other amorphous carbon blacks, may be a consequence of the paramagnetic contribution of surface complexes (e.g., free radicals) which are expected to be predominant on the high area (950 m^2/g) surface of C-1.

TABLE 2

Atomic Absorption Spectroscopic Analysis of Carbolac-1 (C-1)

Impurity	Amount (ppm)[a]
Fe_2O_3	261 (183 for Fe)
SiO_2	81
CaO	5.4
MgO	2.3
Na_2O	nil
K_2O	5.0
MnO	1.8
TiO_2	0.9
Al_2O_3	22
Miscellaneous	71
Total	450

[a] Based on weight.

It is also known that when L_a becomes less than 3.6 nm, the mean diamagnetic susceptibility of a graphitized carbon black begins to decrease as temperature increases (*24*). The variation of susceptibility with temperature for the two carbons is given in Fig. 2. V3G clearly exhibited the temperature-dependent behavior, corresponding to Landau diamagnetism, expected for graphitized carbon blacks. Susceptibility is usually expected to be temperature independent for an amorphous carbon black such as C-1. However, the observed temperature dependence of C-1, which is comparable to that of a normal Curie–Weiss type paramagnetic substance, again suggests the presence of dominant paramagnetic surface complexes.

These magnetic susceptibility data sug-

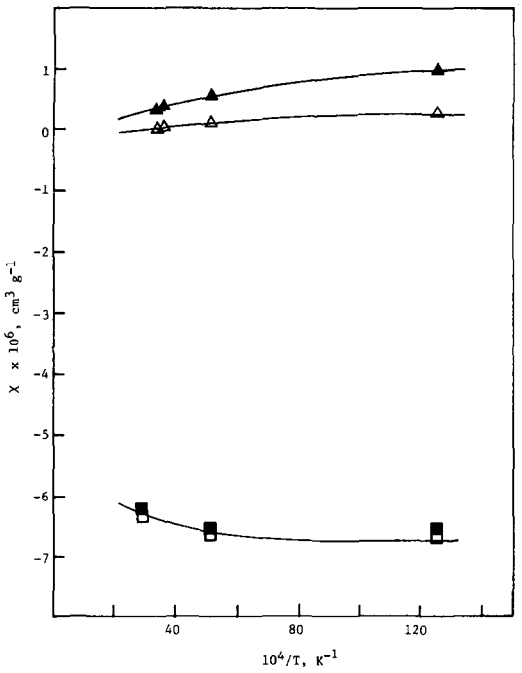

FIG. 2. Diamagnetic susceptibility of carbons as a function of reciprocal temperature. □, V3G unreduced; ■, V3G reduced 1 hr; △, C-1 reduced 1 hr; ▲, C-1 reduced 11 hr.

gest several differences in the characteristics of the two carbon supports. C-1 is amorphous and behaves like an insulator. It is expected that C-1 would have a relatively large number of chemically active surface sites due to its highly disordered structure, and these sites may trap conduction electrons at localized states or may be associated with free radicals (*24*). On the other hand, V3G has electronic properties resembling a conductor due to its itinerant electrons which are free to move throughout the graphitic basal planes. Here crystallite edges and other defects in the graphite may function as the chemically active sites. Hence, the concentration of the active sites in V3G is expected to be much lower than that in C-1. Ehrburger and Walker have studied the size distribution of platinum particles on V3G, and suggested that the extent of heterogeneity of the support is responsible for the different degrees of metal dispersion and resistance to sintering (*25*). By analogy, a higher dispersion and better stability of iron are expected to result with C-1, compared to V3G, due to its greater concentration of active sites and higher surface area. This possibility had already been suggested by the CO chemisorption results. We turn now to discussion of the properties of the iron itself.

C. Mössbauer Studies

The Mössbauer spectra in Fig. 3 show the effects of reduction and subsequent contact with room temperature gases for 4.5% Fe/V3G. The doublet in spectrum 3a is characteristic of ferric iron as expected for the

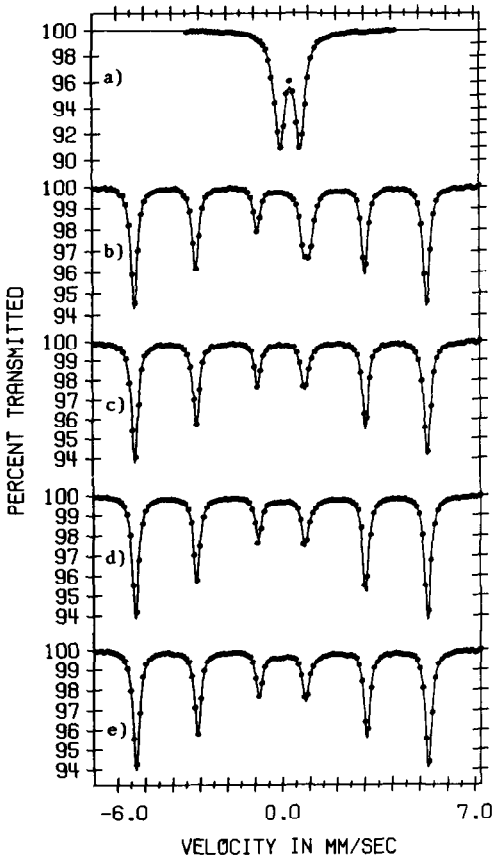

FIG. 3. Room temperature Mössbauer spectra of 4.5% Fe/V3G. (a) Fresh catalyst in He. (b) Reduced in H_2 at 673 K for 1 hr. (c) Reduced in H_2 at 673 K for an additional 15 hr. (d) Exposed to 3.3 H_2/CO for 10 min at 298 K, flushed with He. (e) Exposed to flowing 5% O_2/He at 298 K.

fresh catalyst. Reduction for 1 hr in flowing H_2 at 673 K reduced nearly all the iron to the metallic state, as evidenced by the characteristic six line pattern in spectrum 3b. The area ratios of the lines in this pattern should be 3:2:1:1:2:3. Thus, there is clearly an extra peak in the 1 mm/sec region. As shown in Table 3, a seven line least-squares fit of the data placed the extra peak at 1.06 mm/sec, characteristic of high spin ferrous ion. The presence of this peak indicates that the reduction is not complete after 1 hr at 673 K, but the spectral area attributed to ferrous oxide is only 14%. After an additional 15 hr of reduction in flowing H_2, nearly all the iron is reduced to the metallic state. A slight broadening of peak 4 in spectrum 3c suggests that the maximum spectral area attributable to Fe^{2+} species is <4% of the total area. A short exposure at room temperature of the reduced catalyst to a 3.3 H_2 + CO syngas mixture, followed by a purge with He, caused the appearance of a slight amount of Fe^{3+}, spectrum 3d. More surprising is the result in spectrum 3e, which shows that the sample giving 3d was hardly affected by exposure to 5% O_2/He at room temperature. Since oxygen exposure at room temperature is known to oxidize the iron surface (*26*), spectrum 3e is direct proof that the surface to volume ratio of the iron particles in reduced 4.5% Fe/V3G is very low and that the particles are large.

Figure 4 depicts a second series of experiments on 4.5% Fe/V3G. In this case the reduction was carried out at 723 K. Spectrum 4a shows that the reduction was still incomplete after 1 hr. As shown in Table 3, Fe^{2+} iron still accounts for 12% of the area in this spectrum. Essentially all the iron was reduced to the metallic state after 7 more hr at 723 K in H_2, spectrum 4b. The slight amount of oxidized Fe appearing at 0 and 2 mm/sec could not be computer fitted accurately. After 4 hr of synthesis reaction in 3.3 H_2 + CO at 508 K, much of the iron carburized. Computer fits of spectrum 4c with three magnetically split species showed residual Fe° accounting for 13% of the spectral area, a transition iron carbide with a magnetic field of ~240 kOe and about ~26% of the area (labeled Fe_xC by Niemantsverdriet *et al.* (*27*)), and a major component with a field of about 176 kOe. The relative intensities of the major component were not the 3:2:1:1:2:3 ratios expected for a single species. The size of the magnetic splitting indicates a strong contribution of the iron carbide with H = 173 kOe, called ϵ' by Amelse *et al.* (*28*). The additional intensity in the central region of

TABLE 3

Mössbauer Parameters for Spectra in Figs. 3 and 4

Spectrum	Iron metal				Iron oxide			
	*I*s (mm/sec)	*H* (kOe)	Average width (mm/sec)	Relative area	*I*s (mm/sec)	*Q*s (mm/sec)	Average width (mm/sec)	Relative area
3a					0.36	0.74	0.44	1.0
3b	0.00	330.2	0.28	0.86	1.06	0	0.39	0.14
3c	0.00	330.3	0.29[a]	1.0				
3d	0.00	330.2	0.27	0.93	0.39	1.17	0.76	0.07
3e	0.00	330.2	0.27	0.93	0.41	1.23	0.97	0.07
4a	0.00	330.7	0.27	0.88	1.04	0	0.45	0.12
4b	0.00	330.3	0.27	1.00				
4e	0.00	330.7	0.28	1.00				

[a] Peak 4 had a width of 0.35 mm/sec and 40% more area than peak 3.

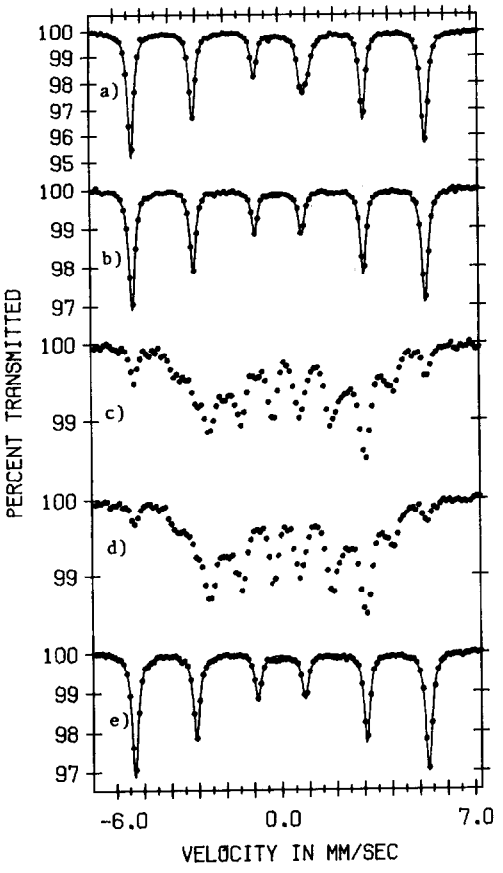

FIG. 4. Room temperature Mössbauer spectra of 4.5% Fe/V3G. (a) Reduced in H_2 at 723 K for 1 hr. (b) Reduced in H_2 at 723 K for 7 additional hr. (c) After 4 hr of reaction at 508 K in 3.3 H_2/CO. (d) After 4 more hr of reaction as in (c). (e) Reduced in H_2 1 hr at 508 K after (d).

the spectrum appears to indicate a small amount of χ carbide. Fitted lines are not drawn through spectra 4c and 4d because complete fits would have required at least 30 lines. The similarity of spectra 4c and 4d, taken after another 4 hr of reaction, indicates that further carburization is a slow process. Spectrum 4e shows that the carburization is easily reversed by treatment in H_2 at reaction temperature. This observation is consistent with the presence of only a minor amount of χ carbide in spectra 4c and 4d since the χ phase is more resistant to hydrogenation (*29*). Exposure of the sample giving spectrum 4e to CO or 5% O_2 in He at room temperature caused negligible changes in the spectra, confirming the large iron particle size in this catalyst.

The behavior of iron in 5.0% Fe/C-1 is markedly different from that in 4.5% Fe/V3G. The iron in a catalyst which had been prereduced at 673 K then passivated in air was Fe^{3+} with a spectrum identical to 3a, but reduction again in H_2 at 673 K for 1 hr gave spectrum 5a for Sample 1. Comparison of spectra 5a and 3b shows that a 1 hr reduction is considerably less effective for 5.0% Fe/C-1 compared to 4.5% Fe/V3G. For 5.0% Fe/C-1, much of the iron remains in the Fe^{2+} state, as indicated by the strong peak at 1.07 mm/sec. Assignment of the species giving the broad shoulder to the left of this peak is difficult because spectral details are not well resolved. This species is reported as Fe* in Table 4. The parameters reported give the best fit but nearly equivalent fits show that Fe* could be Fe^{2+}, Fe^{3+}, or possibly a superparamagnetic carbide. The flatness of the background suggests, however, that there is not a strong superparamagnetic iron carbide or iron metal component. It is important to note the uniqueness of the singlet component at 1 mm/sec. Most Fe^{2+} oxide lines show significant quadrupole splitting. The singlet may indicate an unusually symmetric environment for Fe^{2+} and, thus, suggests that this species is not on a free surface. Though it is not yet possible to model the chemical structure of this catalyst, one might speculate that the Fe^{2+} singlet is related to a support interaction that retards reduction of iron on the C-1 support.

Reduction of 5.0% Fe/C-1 for an additional 16 hr at 673 K gave spectrum 5b. The iron metal peaks are much more intense than in 5a, but a strong peak near 0 mm/sec differentiates this spectrum from its 4.5% Fe/V3G counterpart. The bow in the background of this spectrum indicates the presence of superparamagnetic material. Thus a good fit cannot be expected from simple sums of Lorentzian lines. The parameters in Table 4 show strong contributions of Fe°

TABLE 4

Mössbauer Parameters for Spectra in Figs. 5 and 6

Spectrum	Site	*I*s (mm/sec)	*Q*s (mm/sec)	*H* (kOe)	Average width (mm/sec)	Relative area
5a	Fe°	0.00	—	330.8	0.30	0.20
	Fe^{2+}	1.07	—	—	0.73	0.65
	Fe*	0.25	0.35	—	0.55	0.15
5b	Fe°	0.00	—	328.6	0.36	0.41
	A	0.13	—	—	1.90	0.34
	Fe^{3+}	0.98	2.18	—	0.34	0.23
	B	0.91	0.11	—	0.44	0.02
5c	Fe°	0.00	—	329.8	0.34	0.35
	A	0.11	—	—	1.90	0.34
	Fe^{3+}	0.36	0.89	—	0.60	0.25
	C	0.67	1.52	—	1.01	0.06
5d	Fe°	0.00	—	329.0	0.35	0.15
	Fe^{3+}	0.35	0.89	—	0.72	0.85
6b	Fe°	0.00	—	310.5	0.25	0.06
	ϵ'	0.27	—	160.8	0.55	0.76
	D	0.32	—	212.0	0.53	0.08
	E	0.11	0.67	—	0.42	0.10
6d	Fe°	0.00	—	310.7	0.33	0.20
	Fe^{3+}	0.33	0.82	—	0.61	0.80

and a broad singlet with an isomer shift of 0.13 mm/sec as well as two minor species. These data are not intended to represent a true fit, but to confirm the strong central component and to provide a semiquantitative basis for comparing spectra 5b and 5c. Since both superparamagnetic Fe° and superparamagnetic θ-iron carbide could contribute to species A, an exact assignment cannot be made. Assignment of a critical particle size for superparamagnetism in iron at room temperature is complicated by contributions of particle shape as well as size. For iron on MgO, superparamagnetism has been observed in the size range 1.5–2.5 nm (*3*, *30*).

The sensitivity to oxygen of the highly dispersed iron on C-1 is shown in spectra 5c and 5d. Spectrum 5c shows that at 373 K less than 1 ppm O_2 in He can oxidize 5.0% Fe/C-1. The positions of the two strongest peaks in the center of this spectrum are close to those in spectrum 5b. The more equal intensity of these peaks and their growth relative to the 6 line iron metal pattern identifies them, however, as ferric iron. The fitted parameters in Table 4 strongly support this interpretation. The strong central component, A, is diminished with respect to 5b and the central doublet has parameters characteristic of Fe^{3+}. The unusual parameters for component C are a reminder that the fits are only semiquantitative. The Fe^{3+} parameters are in good agreement, however, with those of spectrum 5d, in which exposure to 5% O_2 in He is shown to carry the oxidation further, affecting most of the iron. The sensitivity to oxidation of iron on Carbolac-1 is clearly in sharp contrast to the behavior of iron on V3G shown in spectrum 3e.

Figure 6 illustrates the effects of the synthesis reaction on fresh unreduced 5.0% Fe/C-1 (Sample 1). Spectrum 6a shows the reduced catalyst after a 16 hr reduction in H at 723 K. The average particle size of iron in this material is lower than that for the prereduced and passivated sample shown in Fig. 5. The greater curvature of the background indicates the presence of more su-

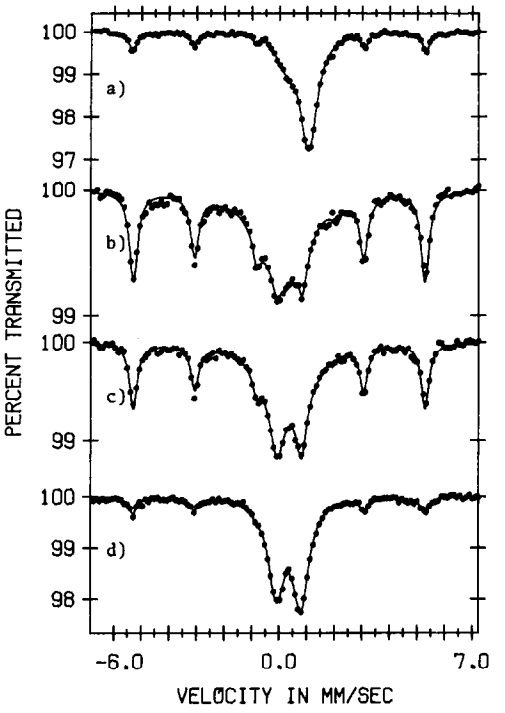

FIG. 5. Room temperature Mössbauer spectra of reduced and passivated 5.0% Fe/C-1. (a) Rereduced in H_2 at 673 K for 1 hr. (b) Reduced in H_2 at 673 K for an additional 16 hr. (c) Heated to 373 K for ½ hr in He. (d) Exposed to 5% O_2/He at 298 K.

perparamagnetic material. This curved background is a property of the sample and not of instrumental origin. The nearly equal intensity of the peaks to the left and right of the peak at zero mm/sec rule out the possibility that the peak at zero is part of a quadrupole doublet. Computer fits to 9 lines gave Fe° with an internal field of 310.6 kOe, a central peak at 0.05 mm/sec, and two very broad peaks forced to fill in the background. In this case the symmetry of the spectrum, low isomer shift of the central peak, and collapse of the Fe field from 330 to 310.6 kOe all strongly support the presence of superparamagnetic Fe°. A careful scan of the ±3 mm/sec region of the spectrum of another reduced sample showed a small peak characteristic of magnetically split θ-carbide, but its intensity indicated that well below 5% of the iron was in this form.

As shown in spectrum 6b, 6 hr of synthesis of 3.3 H_2 + CO at 508 K converted most of the iron to ϵ' carbide, the phase expected at this temperature (*27*). The 20 line computer fit to this spectrum (Table 4) shows that all the magnetic fields are decreased from their expected values and that an additional doublet is needed in the center to account for the high intensity of the innermost pair of peaks. This behavior is consistent with the presence of small particles and the onset of superparamagnetism (*31–33*). In this case the central doublet appears to be superparamagnetic ϵ' iron carbide (*28*), but again the onset of superparamagnetism lowers the reliability of the computer fits. The reversibility of the carburization by H_2 at reaction temperature is illustrated in spectrum 6c. Subsequent exposure of that sample to O_2 converted most of the iron to Fe^{3+}, as shown by the narrow doublet in

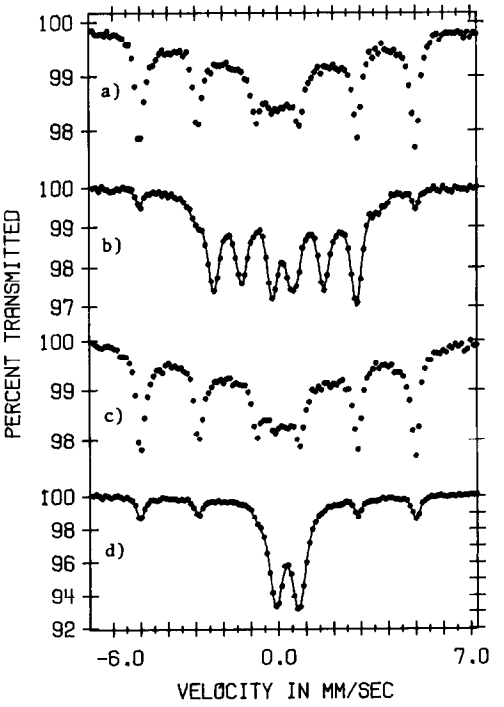

FIG. 6. Room temperature Mössbauer spectra of 5.0% Fe/C-1. (a) Reduced in H_2 at 723 K for 16 hr. (b) After 6 hr of reaction at 508 K in 3.3 H_2/CO. (c) Rereduced in H_2 at 508 K for 8 hr. (d) Slowly passivated by adding pulses of O_2 to flowing He.

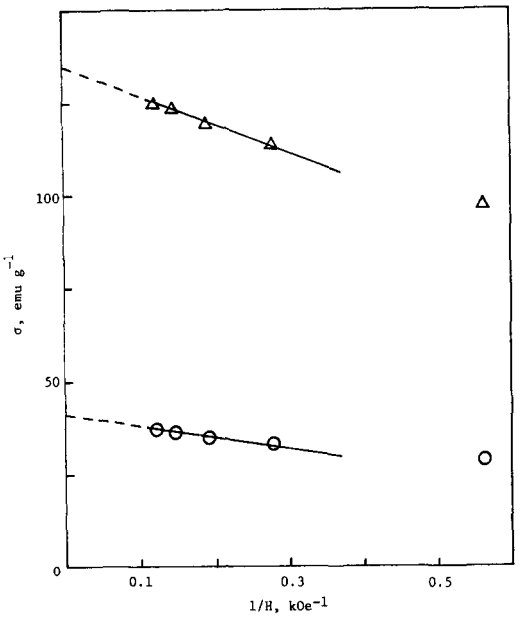

FIG. 7. Saturation magnetization of carbon-supported iron (reduced 1 hr at 673 K). O, 5.0% Fe/C-1; Δ, 4.5% Fe/V3G.

spectrum 6d, and confirmed the high dispersion of the iron.

The important conclusions from the Mössbauer studies for Fe on C-1 and V3G can be summarized in two statements. Iron on V3G is in large particles and exhibits bulk iron behavior. Iron on Carbolac-1 is highly dispersed, is extremely sensitive to reoxidation even by traces of oxygen, and shows an altered reducibility suggestive of support interaction. In seeking the chemical origins of the activity maintenance of the Fe/C-1 catalyst, one is drawn immediately to the unusually small iron particle size. The influences of the ϵ' carbide phase, its particle size, and possible support interaction all merit further investigation.

D. Magnetization Measurements

Per gram magnetization (σ, emu g^{-1}) of iron on 5.0% Fe/C-1 and 4.5% Fe/V3G was measured as a function of the field strength at 80 K, after the catalysts were reduced in flowing H_2 for 1 hr at 673 K. The saturation magnetization (σ_S) was estimated by plotting σ measured at 80 K versus $1/H$ and extrapolating to zero, as shown in Fig. 7. For iron particles of diameters greater than 2 nm, σ_S can be accurately estimated by linear extrapolations of data taken at fields greater than 10 kOe ($1/H$ = 0.1 kOe^{-1}); some workers (*3*) have obtained values for σ_S with fields up to only 3.06 kOe. Since pure bulk iron has a saturation magnetization of 220 emu/g at 80 K, the results in Fig. 7 suggest that the fraction of iron existing as reduced metal after the pretreatment is 0.19 for 5.0% Fe/C-1 and 0.61 for 4.5% Fe/V3G. Increased reduction times did not alter these values significantly; however, all runs included a 1 hr evacuation at 650 K followed by cooling *in vacuo*, prior to magnetic measurements. The conflict between these results and those from the Mössbauer studies can best be resolved by assuming that some reoxidation occurred during the magnetization measurements. The Mössbauer measurements demonstrate that 5.0% Fe/C-1 is highly susceptible to oxidation by trace amounts of O_2 ($\leq$1 ppm). The incomplete reduction of 4.5% Fe/V3G suggests an exposure to oxygen at high temperature, perhaps during outgassing or when He was added to facilitate cooling, as Mössbauer measurements indicate 86% reduction after this pretreatment. The magnetization experiments are especially sensitive to small amounts of oxygen because the Faraday method requires very small (1 mg) catalyst samples and the dead volume is very large in the Cahn microbalance.

Small particles of a ferromagnetic (or ferrimagnetic) substance exhibit superparamagnetism when they exist below the critical size required for a single magnetic domain (*34, 35*). An operational definition of superparamagnetism is that a good superposition of data points is obtained for the relative magnetization (σ/σ_S) plotted versus (H/T_m), where T_m is the temperature at which the measurement is made. No hysteresis is observed in this case whereas it is observed for the corresponding bulk material. The magnetization curves of iron in

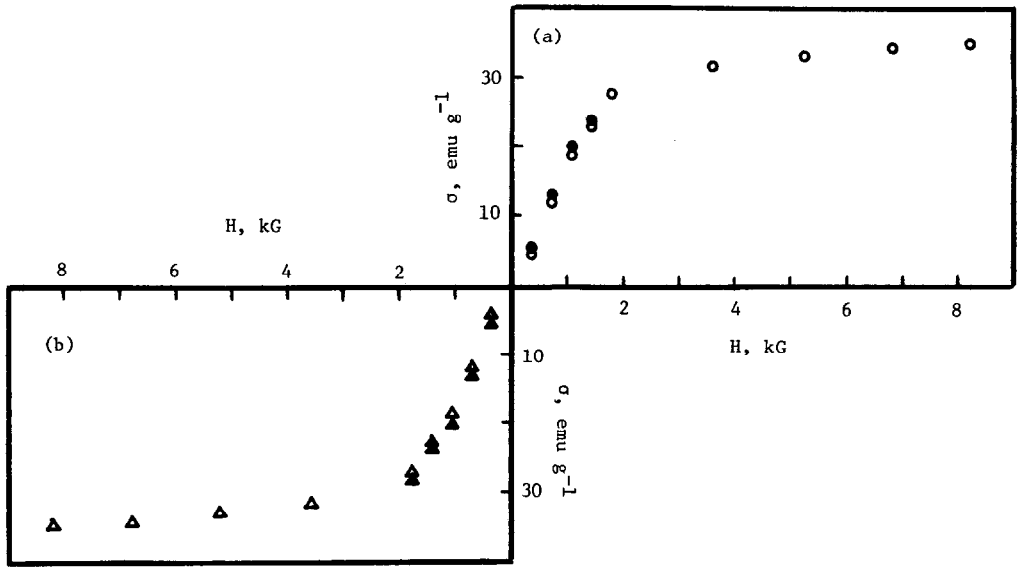

FIG. 8. Magnetization per gram iron for 5.0% Fe/C-1 in He (T = 80 K). (a) Initial run measured in a sequence of increasing (○) and decreasing (●) field. (b) Duplicated run measured after reversing the polarity of the magnets in a sequence of increasing (△) and decreasing (▲) field.

5.0% Fe/C-1 measured at temperatures between 80 and 300 K showed no hysteresis. This behavior is illustrated by the magnetization data measured at 80 K shown in Fig. 8. Based on a magnetization relaxation time of $\tau = 10^2$ sec, iron particles of diameters less than 7.7 nm show no hysteresis at 80 K (*35*). In addition, Fig. 9 shows a reasonable superposition of σ/σ_S curves for the data at 195 and 295 K within the limits of experimental error. The lack of superposition of the data points at 80 K suggests that the

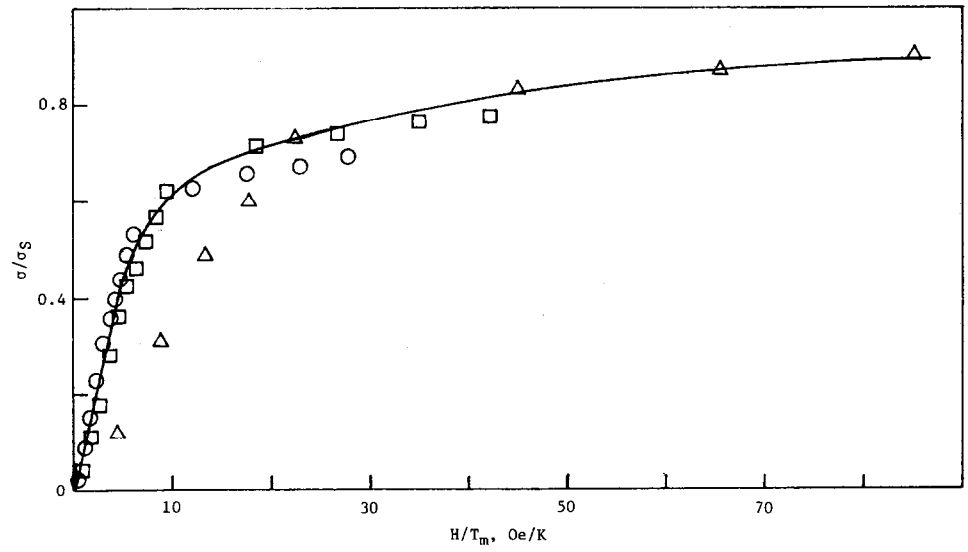

FIG. 9. Relative magnetization measurements at various temperatures for 5.0% Fe/C-1. ○, 295 K; □, 195 K; △, 80 K.

system has a blocking temperature, T_B, somewhere between 80 and 195 K. Above T_B the thermal fluctuations become dominant and lead to good superparamagnetic behavior as discussed. Therefore, it is concluded that the iron particles in Fe/C-1 are small enough to behave superparamagnetically. From the top superparamagnetic curve in Fig. 9, it is possible to estimate the upper and lower limits of the iron particle size, d, using the low field (d_{LF}) and high field (d_{HF}) approximations of the Langevin function (*36*):

$$d_{LF}^3 = \frac{18k}{\pi I_S}(\sigma/\sigma_S)/(H/T_m); \quad \text{Low field approximation} \quad (3)$$

$$d_{HF}^3 = \frac{6k}{\pi I_S}[1 - (\sigma/\sigma_S)]^{-1}/(H/T_m); \quad \text{High field approximation} \quad (4)$$

where k is the Boltzmann constant and I_S is the spontaneous magnetization per unit volume for the bulk material.

The difficulty with trace amounts of oxygen does not prevent the estimation of iron particle size as we can consider three possible phases which could exhibit such behavior: Fe° (Case I), γ-Fe_2O_3 (Case 2), and Fe_3O_4 (Case 3). The spontaneous magnetizations are 1707, 417, and 480 kOe, respectively. The upper and lower limits of the iron particle size, estimated for each case by substituting the corresponding I_S value into Eqs. (3) and (4), are presented in Table 5. The d_{LF} and d_{HF} values agree well with each other and fall in the 2–5 nm range. When γ-Fe_2O_3 or Fe_3O_4 is reduced to Fe°, the iron particle size would become about $\frac{3}{4}$ of the size of the iron oxide particles; therefore, the metallic iron particle sizes for Cases 2 and 3 are in much better agreement with Case 1 than they appear to be. These magnetic results thus confirm that the average iron particle size for 5% Fe/C-1 is very small, regardless of its oxidation state. It must be noted, however, that this particle-size information is valid only for the fraction of the iron which is responsible for the magnetization of the sample.

TABLE 5

Metal Particle Size for Catalyst A (5.0% Fe/C-1)

Reduction[a] time (hr)	Metal particle size (nm) for					
	Case 1 (Fe°)		Case 2 (γ-Fe_2O_3)		Case 3 (Fe_3O_4)	
	d_{LF}	d_{HF}	d_{LF}	d_{HF}	d_{LF}	d_{HF}
1	3.3	2.6	5.3	4.2	5.0	4.0
11	3.3	2.7	5.3	4.3	5.0	4.1
11 + 4.5[b]	3.4	2.7	5.4	4.3	5.2	4.1

[a] Reduced in a H_2 flow of 100 cm^3/min^{-1} at 673 K.
[b] Reduced additionally for 4.5 hr at 723 K.

For 4.5% Fe/V3G, as shown in Fig. 10, hysteresis was evident even at room temperature, suggesting the presence of large multidomain ferro- or ferrimagnetic (i.e., Fe°, γ-Fe_2O_3, or Fe_3O_4) particles. It was also observed that the sample became permanently magnetized after exposure to high fields, and it could be demagnetized only by heating to a high temperature. Based on a magnetization relaxation time of $\tau = 10$ sec, metallic iron (Fe°) particles of diameters greater than 25 nm show hysteresis at room temperature. Furthermore, the σ/σ_S versus H/T_m curves for 4.5 Fe/V3G showed no superposition. It is thus concluded that most of the iron in the V3G catalyst exists as large multidomain ferromagnetic particles, which is in excellent agreement with chemisorption, Mössbauer, and X-ray results. Despite the uncertainties regarding the iron phases present in the catalyst samples during the magnetization measurements, the average particle sizes estimated from the magnetic data clearly support the conclusion that the average iron particle size for 5.0% Fe/C-1 is at least an order of magnitude smaller than that for 4.5% Fe/V3G.

E. Catalytic Behavior

The kinetic behavior for CO hydrogenation over carbon-supported catalysts has been described elsewhere (*1*, *2*). The activi-

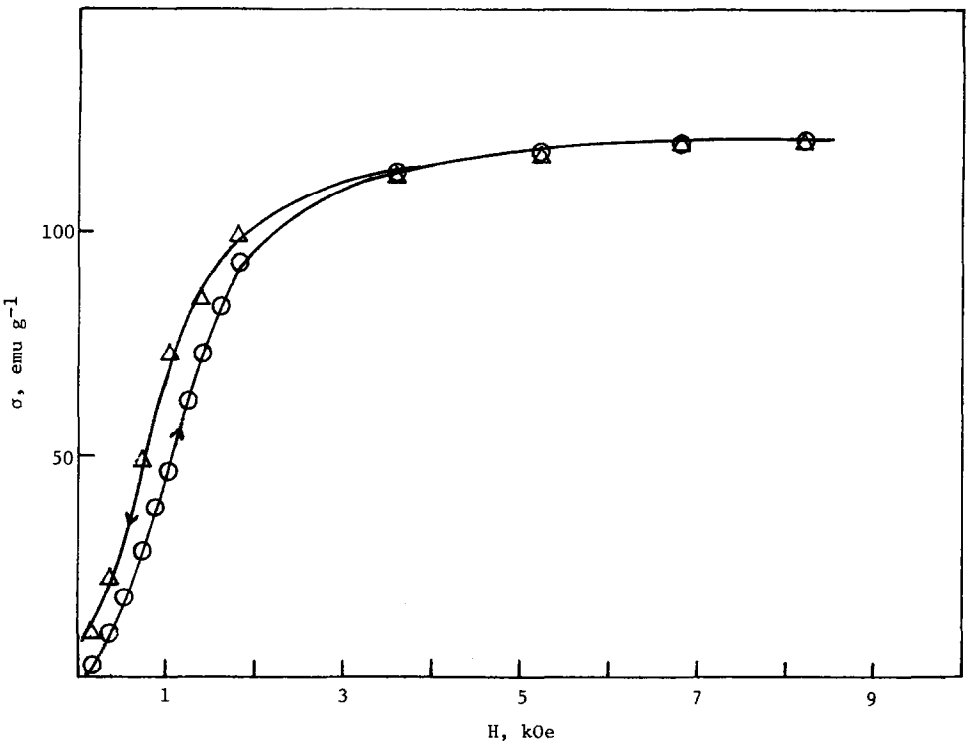

FIG. 10. Magnetization per gram iron for 4.5% Fe/V3G in helium (T = 295 K).

ties of the catalysts prepared in this study were orders of magnitude higher than those reported for other iron/carbon systems (*37, 38*), and are comparable to or higher than those for Fe/Al_2O_3 catalysts on a per gram Fe basis. These studies also showed that turnover frequency (TOF) values were strongly dependent on dispersion, with TOF being an order of magnitude lower on small Fe particles than on large (~30 nm) iron crystallites (*2*). A similar trend was reported by Storm and Boudart for MgO-supported iron (*39*). It was because of this behavior that a low-dispersion (LD) catalyst (4.5% Fe/V3G) and a high-dispersion (HD) catalyst (5.0% Fe/C-1) were chosen for further characterization. Table 6 shows that the large difference in TOF exists regardless of choice of CO uptake (195 vs 300 K) and that the activities on large Fe crystallites on carbon and alumina are very similar. The CO adsorption at 195 K is expected to be the best measure of the reduced iron surface (*3, 10*). More intriguing aspects of the HD group of carbon-supported iron catalysts include a much higher olefin/paraffin ratio and essentially no deactivation during long periods of continuous operation (*1, 2*).

The marked inhibition of hydrogen chemisorption on these HD iron catalysts could easily be responsible for the lower turnover frequencies because CO hydrogenation has a first-order dependence on hydrogen pressure (*2*). Lower surface concentrations of hydrogen would reduce the hydrogenation capability of the catalyst thereby giving higher olefin/paraffin ratios and lower methane make. However, the excellent activity maintenance would not be expected to be a consequence of lower concentrations of surface hydrogen and, at this time, appears to be a result of the rapidity of formation of the transition iron carbides and their stabilization on the carbon support. Although a strong interaction may exist between the iron and the C-1 surface, which results in

TABLE 6

Influence of Particle Size on Turnover Frequencies (TOF) at 548 K

Catalyst	Activity (μmole s^{-1} g Fe^{-1})		TOF—CH_4 ($s^{-1} \times 10^3$)		TOF—CO ($s^{-1} \times 10^3$)		Diameter (nm)	
			[a]	[b]	[a]	[b]	[a]	[b]
	CH_4	CO						
5.0% Fe/C-1 Sample I	18	69	2.5	7.1	9.3	26	1.0	2.7
4.5% Fe/V3G	13	69	107	60	554	310	54	33
10% Fe/Al_2O_3	6.1	16	58	—	152	—	64	—

[a] Based on CO adsorption at 300 K.
[b] Based on CO adsorption at 195 K.

the formation of small iron clusters and their stabilization under reaction conditions, future studies are needed to determine whether the different adsorption and catalytic behavior of the 5.0% Fe/C-1 is due primarily to a crystallite size effect or to a metal-support interaction. The results of this study combined with those of Storm and Boudart and of Topsøe *et al.* on MgO-supported iron suggest, however, that crystallite size has a very pronounced effect in iron catalysts for CO hydrogenation.

SUMMARY

Chemisorption, Mössbauer effect, magnetic studies, and kinetics have been combined to characterize iron on V3G, a low surface area graphitic carbon, and on Carbolac-1, a porous, high surface area carbon black. Magnetic studies confirm the conducting, graphitic properties of V3G and the insulating, amorphous properties of Carbolac-1. All techniques show the iron on V3G to be in large particles which behave normally. The iron on Carbolac-1 is highly dispersed, shows superparamagnetism and oxidation sensitivity characteristic of very small particles, and exhibits a decreased reducibility suggestive of a support interaction. These small iron particles show greatly decreased H_2/CO chemisorption ratios at temperatures up to 473 K, a high olefin to paraffin ratio, and excellent activity maintenance during Fischer–Tropsch synthesis. These properties appear to be a consequence of an iron crystallite size effect; however, the role of the carbon is not clear and an interaction between the iron and the carbon surface may exist which creates and stabilizes these small iron and iron carbide crystallites.

ACKNOWLEDGMENTS

We are grateful to the National Science Foundation for support of this work through Grants DMR 77-23798 and CPE-7915761. The latter grant is co-sponsored by the Army Research Office. We also thank Conoco, Inc. for support through a grant to the Coal Research Center at Purdue University and D. J. Knoechel for his able assistance in computer fitting the Mössbauer data.

REFERENCES

1. Vannice, M. A., Walker, P. L., Jung, H-J., Moreno-Castilla, C., and Mahajan, O. P., *Proc. VII Int. Cong. Catal., Tokyo*, Paper A31, p. 460 (1980).
2. Jung, H-J., and Vannice, M. A., *J. Catal.*, accepted for publication.
3. Boudart, M., Delbouille, A., Dumesic, J. A., Khammouma, S., and Topsøe, H., *J. Catal.* **37**, 486 (1975).
4. Vannice, M. A., *J. Catal.* **37**, 449 (1975).
5. Mulay, L. N., "Magnetic Susceptibility." Reprint Monograph, Wiley Interscience, New York, 1966; Krieger Publishers, Melbourne, Fla.
6. Mulay, L. N., *in* "Physical Methods of Chemistry" (A. Weissberger and W. Rossiter, Eds.), Ch. 7. Wiley-Interscience, New York, 1972.
7. Mulay, L. N., and Boudreaux, E. A. (Eds.) (a) "Theory and Applications of Molecular Diamagnetism" and (b) "Theory and Applications

of Molecular Paramagnetism." Wiley-Interscience, New York, 1976.
8. Raupp, G. B., and Delgass, W. N., *J. Catal.* **58,** 337 (1979).
9. Delgass, W. N., Cheng, L. Y., and Vogel, G., *Rev. Sci. Instrum.* **47,** 968 (1976).
10. Emmett, P. H., and Brunauer, S., *J. Amer. Chem. Soc.* **59,** 319 (1937).
11. Wedler, G., Geuss, K. P., Colb, K. G., and McElhiney, G., *Appl. Surface Sci.* **1,** 471 (1978).
12. Wedler, G., Colb, K. G., McElhiney, G., and Heinrich, W., *Appl. Surface Sci.* **2,** 30 (1978).
13. Broden, G., Gafner, G., and Bonzel, H. P., *Appl. Phys.* **13,** 333 (1977).
14. Rhodin, T. N., and Brucker, C. F., *Sol. St. Comm.* **23,** 275 (1977).
15. Textor, M., Gay, I. D., and Mason, R., *Proc. R. Soc. London A* **356,** 37 (1977).
16. Topsøe, H., Topsøe, N., and Bohlbro, H., *Proc. VII Int. Cong. Catal.*, p. 247.
17. Farrauto, R. J., *AIChE Symp. Ser.* **70,** 163 (1974).
18. Jung, H-J., Ph.D. Thesis, The Pennsylvania State University (1981).
19. Emmett, P. H., and Takezawa, N., *J. Res. Inst. Catal., Hokkaido Univ.* **26-1,** 37 (1978).
20. Bartholomew, C. H., and Pannell, R. B., *J. Catal.* **65,** 390 (1980) and references therein.
21. Honda, K., *Ann. Phys. Lpz.* **32,** 1068 (1910).
22. Owen, M., *Ann. Phys. Lpz.* **37,** 657 (1912).
23. Pacault, A., *Carbon* **12,** 1 (1974).
24. Marchand, A., *Chem. Phys. Carbon* **7,** 155 (1971).
25. Ehrburger, P., and Walker, P. L., Jr., *J. Catal.* **55,** 63 (1978).
26. Brundle, C. R., Chuang, T. J., and Wandelt, K., *Surface Sci.* **68,** 459 (1977).
27. Niemantsverdriet, J. W., Van der Kraan, A. M., van Dijk, W. L., and van der Baan, H. S., *J. Phys. Chem.* **84,** 3863 (1980).
28. Amelse, J. A., Butt, J. B., and Schwartz, L. H. *J. Phys. Chem.* **82,** 558 (1978).
29. Goodwin, J. G., and Parravano, G., *J. Phys. Chem.* **82,** 1040 (1978).
30. Topsøe, H., Dumesic, J. A., Derouane, E. G., Clausen, B. S., Mørup, S., Villadsen, J., and Topsøe, N., *in* "Preparation of Catalysts II" (B. Delmon, P. Grante, P. A. Jacobs, and G. Poncelet, Eds.), p. 365. Elsevier, Amsterdam, 1979.
31. Mørup, S., and Topsøe, H., *Appl. Phys.* **11,** 63 (1976).
32. Mørup, S., Topsøe, H., and Lipka, J., *J. Phys.* **37,** C6-287 (1976).
33. Phillips, J., Clausen, B., and Dumesic, J. A., *J. Phys. Chem.* **84,** 1814 (1980).
34. Selwood, P. W., "Chemisorption and Magnetism." Academic Press, New York, 1975.
35. Jacobs, I. S., and Bean, A. P., *in* "Magnetism" (G. T. Rado and H. Suhl, Eds.), Vol. III, Ch. 6. Academic Press, New York, 1963.
36. Yamamura, A., and Mulay, L. N., *J. Appl. Phys.* **50,** 7795 (1979); also see Ref. (35).
37. Kikuchi, E., Ino, T., Ito, N., and Morita, Y., *Bull. Japan. Petr. Inst.* **18,** 139 (1976).
38. Parkash, S., and Chakrabartty, *Carbon* **16,** 231 (1978).
39. Storm, D., and Boudart, M., 6th North Amer. Catal. Soc. Meeting, Chicago, March 1979.